

Anti-breast cancer effect and mechanism of ethyl acetate extract of persimmon leaves

Fang Zhuge

Guangxi University of Chinese Medicine

Xiusha Wei

Guangxi Medical University

Yani Wu

Guangxi Medical University

Guining Wei

Guangxi Medical University

Ming Chen

Guangxi Medical University

Yutong Gao

Guangxi Medical University

Zhaoni Chen

Guangxi Medical University

Xiaolin Zhang

Guangxi Medical University

Shunyu Lu

Guangxi Medical University

Renbin Huang

Guangxi Medical University

Xiuneng Tang (✉ zhugexiaozhu@163.com)

Maternal and Child Health Hospital of Guangxi Zhuang Autonomous Region

Research

Keywords: PLE, Anti-breast cancer, Mechanism of action, apoptosis and antiproliferative, MAPK signaling pathway

Posted Date: December 23rd, 2020

DOI: <https://doi.org/10.21203/rs.3.rs-132197/v1>

License:   This work is licensed under a Creative Commons Attribution 4.0 International License.

[Read Full License](#)

Abstract

Aim: The anti-breast cancer effect and mechanism of ethyl acetate extract of persimmon leaves (PLE) were determined.

Methods: Persimmon leaves were extracted by reflux at 80°C with 80% ethanol as the solvent. The total extracts of persimmon leaves were extracted with ethyl acetate, and the yield was calculated by weighing. The mouse breast cancer cell line 4T1 was cultured in vitro, and different concentrations of PLE were added. At the same time, the effects of PLE at different concentrations (25, 50, 100 µg/ml) on cell apoptosis ability were detected by Acridine Orange and Ethidium Bromide (AOEB) and flow cytometry experiments. In addition, real-time quantitative PCR (real-time PCR, RT-PCR) was used to test the expression of the Bax, Bcl-2, ERK1/2, MEK1/2 and RAF genes. In vivo tumor-bearing mouse model: A breast cancer transplant tumor model was established with BALB/c mice. The doses of PLE were 30, 60 and 120 mg/kg body weight/d, and the dose of CTX was 20 mg/kg body weight/d. The tumor inhibition rate and the effects of PLE on immune organs in tumor-bearing mice with 4T1 breast cancer were determined. The expression levels of IL-6, TNF- α , TGF- β and VEGFA in the serum of mice were detected by ELISA. The expression of the Bax, Bcl2, ERK1/2, MEK1/2 and RAF genes was determined by RT-PCR. The protein expression levels of Bax, Bcl-2, Caspase-3, p-MEK, p-JNK and p-P38 in tumor tissues were detected by immunohistochemistry. In addition, the protein expression levels of MAPK pathway components were assessed through Western blotting.

Results: A total of 119.34 g ethyl acetate extract was obtained from 3 kg persimmon leaves with a yield of 3.98%. In vitro: MTT results indicated a strong antiproliferative effect of PLE on breast cancer cell lines. AOEB and flow cytometry assays showed that PLE promoted the apoptosis of breast cancer cells. PCR results showed that PLE could inhibit Bcl-2, promote Bax expression, and downregulate ERK1/2, MEK1/2, and RAF gene expression. In vivo: PLE had a significant inhibitory effect on breast cancer, and the tumor inhibition rates were 11.65%, 33.71% and 47.24% from low dose to high dose, respectively, showing a concentration dependence. The tumor inhibition rate of CTX was 57.74%. Meanwhile, PLE can increase the spleen and thymus index of 4T1 mice and decrease the liver index of 4T1 mice. Compared with the model group, PLE significantly reduced the expression levels of IL-6, TNF- α , TGF- β and VEGFA in the serum of mice. PCR results showed that PLE could inhibit Bcl-2, promote Bax expression, and downregulate ERK1/2, MEK1/2, and RAF gene expression. Immunohistochemical results showed that the PLE group and CTX group significantly promoted the expression of Bax and Caspase-3 proteins and downregulated the expression of Bcl-2, p-MEK, p-JNK and p-P38 proteins. WB results showed that PLE regulated the expression of proteins in the MAPK pathway.

Conclusion: PLE enhances immunity, inhibits angiogenesis, inhibits 4T1 cell proliferation and induces apoptosis. Its apoptosis mechanism is related to the regulation of Bax/Bcl-2/Caspase-3 protein and the phosphorylation of regulatory proteins related to the MAPK signaling pathway.

1. Introduction

Cancer is considered the second leading cause of death worldwide after cardiovascular diseases^[1]. Despite the tremendous improvements in cancer therapy over the past decade, breast cancer estimated death is still considered the second most common in the world after lung cancer^[2, 3]. Current therapeutic treatments for cancer usually cause serious side effects, such as bladder, kidney, lung or heart damage. Thus, the development of effective drugs with fewer adverse effects for the chemopreventive intervention of cancers is the top priority in cancer research^[4]. Studies are continuously being conducted in the search for novel effective and nontoxic anticancer compounds from various medicinal plants^[5]. Persimmon (*Diospyros kaki L.*) is a native Chinese plant that is widely found in tropical and subtropical eastern Asia^[6]. It has been reported that persimmon leaves have anti-tumor^[7], hypoglycemic^[8], antioxidant^[9], anti-inflammatory^[10], antibacterial^[11], and antihypertensive^[12] properties. In this study, we mainly studied the effect and mechanism of ethyl acetate extract of persimmon leaves (PLE) on breast cancer.

2. Materials And Methods

2.1 Reagents and chemicals

PLE was received from Lingshan County, Guangxi Autonomous Region, China, and persimmon leaves were isolated from 80% aq. All other chemicals and solvents used in this study were provided by Sangon Biotech (Shanghai), Co., Ltd.

2.2 Cell experiments

2.2.1 Cell culture

The 4T1 breast cancer cell line was purchased from Shanghai Institute of Biochemistry and Cell Biology. Cells were cultured in RPMI 1640 with 10% FBS (v/v) medium in a 5% CO₂ atmosphere in a 37 °C incubator with the medium changed every 2 days; they were passaged once every 3–4 days. The cells in the exponential growth stage were moderately digested with trypsin, and after centrifugation of the cell suspension, the supernatant was discarded. The cells were resuspended in PBS, and the concentration of the cell suspension was adjusted to 1 × 10⁶/mL for tumor inoculation.

2.2.2 MTT assay

4T1 cells were seeded in 96-well plates at a density of 3 × 10³ cells/well in 100 μl culture medium/well. After 24 h incubation, cells were treated with different formulations at gradient concentrations of PLE (0, 10, 20, 30, 40, 50, 60, 70, 80, 90, and 100 μg/ml). After 24 h of incubation at 37 °C, 100 μl MTT reagent (0.5 mg/ml) was added to each well, and the cultures were incubated for an additional 4 h. The MTT reagent was removed and replaced by DMSO to ensure that solubilization was complete. Absorbance at 470 nm was measured on a microplate reader. Half-maximal inhibitory concentration (IC₅₀) values were calculated from fitted response curves of the concentration and viability (%). The IC₅₀ was calculated according to the linear regression method of SPSS 21.0.

2.2.3 AOEB assay

4T1 cells growing in a logarithmic period were inoculated in a 6-well plate at a density of 1×10^5 /well. Each well was 2 ml, and 3 secondary wells were set in each well. The 6-well plate was placed in a 5% CO₂ incubator at 37 °C for routine culture. After the cells had grown to almost confluence, the original medium was absorbed, and 2 ml of medium containing different concentrations was added to each well (0, 25 µg/ml, 50 µg/ml, and 100 µg/ml). After 24 h of incubation, the medium was removed and washed with PBS. Then, 1 ml PBS and 20 µl AOEB (AO: EB = 1:1) were added. After 3–5 min, the cells were placed under a fluorescence microscope to observe the morphological changes of apoptotic cells and to take photos.

2.2.4 Flow cytometry

4T1 cells (2×10^5 cells/well) were plated onto 6-well plates and incubated for 24 h. Then, cells were treated with different formulations of gradient concentrations of PLE (0, 25 µg/ml, 50 µg/ml, and 100 µg/ml). After 24 h of incubation, the cells were treated, stained with an apoptosis detection kit, and measured by flow cytometry.

2.2.5 Real-time polymerase chain reaction(RT-PCR)

4T1 cells (2×10^5 cells/well) were plated onto 6-well plates and incubated for 24 h. Then, cells were treated with different formulations of gradient concentrations of PLE (0, 25 µg/ml, 50 µg/ml, and 100 µg/ml). After 24 h of incubation, the cells were treated, and a TRIzol kit (Invitrogen) was used to extract RNA from cells, which was reverse-transcribed into cDNA using a Transcriptor First Strand cDNA Synthesis Kit (Roche, USA) following the manufacturer's instructions. RT-PCR was performed using a 7300 real-time PCR detection system (Applied Biosystems, Foster City, CA, USA). The expression level of the indicated genes was analyzed using $2^{-\Delta\Delta Ct}$. GAPDH was used as a control. The sequences of the primers are shown in Table 1.

Table 1
Primer information for the real-time PCR

Gene	Forward primer(5'-3')	Reverse primer(5'-3')
RAF	ACTGTGGTCAATGTGCGGATGG	GGCGGCATCGGTGTTCCAATC
MEK1	GACTTTGAGAATCAGCGAAC	GTTTGATCTCCAGGTGGATCAG
MEK2	CATCAGTGTAGGTCATGGGATG	GTGGCTCGTTCACTATGTAGTC
ERK1	CTGCTGGACCGGATGTTAACCTTC	ACTGGCTCATCTGTCCGGATCGTAG
ERK2	ATCTCAACAAAGTTCGAGTTGC	GTCTGAAGCGCAGTAAGATTTT
Bcl-2	GATGACTTCTCTCGTCGCTAC	GAACTCAAAGAAGGCCACAATC
Bax	TTGCCCTCTTCTACTTTGCTAG	CCATGATGGTTCTGATCAGCTC
GADPH	GGTTGTCTCCTGCGACTTCA	TGGTCCAGGGTTTCTTACTCC

2.3 Animal experiments

BALB/c female mice (5–6 weeks old) were obtained from the Model Animal Research Centre of Changsha University (Changsha, China). Mice were maintained in an SPF-level animal center with a controlled temperature of 20 °C-25 °C, 48%–52% humidity and a 12 h light-dark cycle at Guangxi Medical University. All experiments were performed with approval from the Institutional Animal Care and Use Committee of Guangxi Medical University. Animal ethics review followed the Guiding Opinions on the Treatment of Laboratory Animals issued by the Ministry of Science and Technology of the People's Republic of China and the Laboratory Animal Guideline for Ethical Review of Animal Welfare issued by the National Standard GB/T35892-2018 of the People's Republic of China. After 7 days of adaptive feeding, under the right axillary of 60 BALB/c mice, 0.2×10^6 4T1 cells were injected. The cancer cells were inoculated subcutaneously for 5 days. Sixty successful model mice were randomly selected for weighing and recorded, and then randomly divided into five groups: model control group, low dose group (30 mg/kg), medium dose group (60 mg/kg) and high dose group (120 mg/kg) of PLE and positive control group (CTX, 20 mg/kg). In addition, 12 unmodeled mice were randomly selected as the blank control group. The water supply in the blank control group and the model group was 20 ml/kg per day. After 14 days, the mice were killed and weighed. Serum was collected from each group in parallel, thymus, spleen and liver tissues were taken, and tumor blocks were stripped and weighed.

2.3.1 Removal of the tumor and spleen

The mice were sacrificed, and the tumor tissues and thymus, spleen and liver tissues were collected under aseptic conditions. The tumor inhibition rate and the index of each organ were calculated.

2.3.2 Detection of cytokines in serum

ELISA kits were used to determine the levels of cytokines (IL-6, TNF- α , TGF- β and VEGFA) in the serum samples. The procedure for the experiment was carried out according to the kit instructions.

2.3.3 Real-time polymerase chain reaction (RT-PCR)

Total RNA was extracted from tumors in mice by using TRIzol (Invitrogen, Carlsbad, CA, USA) according to the manufacturer's instructions, and the RNA was reverse transcribed to complementary DNA (cDNA) using the PrimeScript RT reagent kit and gDNA Eraser. The sequences of the primers are shown in Table 1. RT-PCR was performed using a 7300 real-time PCR detection system (Applied Biosystems, Foster City, CA, USA). GAPDH was used as a reference gene. The results of the real-time PCR were calculated by the $2^{-\Delta\Delta C_t}$ method.

2.3.4 Immunohistochemistry

Immunohistochemistry analysis was performed to detect the expression of Bax, Bcl-2, Caspase-3, p-MEK, p-JNK and p-P38 in tumor tissues. The sections were dewaxed, and the antigen was repaired with citric acid solution (0.01 mol/L, pH 6.0), after which the sections were incubated with 3% H₂O₂. The sections were blocked with nonimmunoreactive sera and then incubated with antibodies against Bax, Bcl-2, Caspase3, p-MEK, p-JNK and p-P38 overnight at 4 °C. The next day, the sections were incubated with goat anti-rabbit (HRP), stained with DAB chromogen and counterstained with hematoxylin. The sections were observed and analyzed using a light microscope (Olympus, Tokyo, Japan).

2.3.5 Western blotting

Western blotting was performed to analyze the expression of MAPK signaling pathway-related proteins in the tumor tissues of mice. Proteins were extracted from tumor tissue by grinding with liquid nitrogen and adding lysis buffer, PSMF and phosphatase inhibitors. Equal amounts of proteins were mixed with 4 × loading buffer after measuring the protein concentrations using a BCA assay. The proteins were separated by 10% SDS-PAGE and then transferred to a PVDF membrane. Subsequently, the membranes were blocked with 5% nonfat milk for 1 h and then incubated with primary antibodies overnight at 4 °C. Then, the membranes were incubated with anti-rabbit IgG (H + L) secondary antibodies at room temperature for 1 h. The Western blotting results were detected and analyzed using Image Studio Lite.

3. Results

3.1 The yield of PLE

A total of 119.34 g ethyl acetate extract was obtained from 3 kg persimmon leaves with a yield of 3.98%.

3.2 PLE proliferation inhibition of 4T1 cells

We examined the cell proliferation of 4T1 cells by the MTT assay. Our data showed that cell proliferation was significantly reduced in 4T1 cells after 24 h of incubation ($p < 0.01$) (Table 2), indicating that the

expression level of 4T1 was important in regulating cell proliferation. The IC₅₀ value of frullanolide for the breast cancer cell lines was 50.02 ± 1.69 µg/ml.

Table 2
Inhibition rate of PLE on 4T1

Group	Concentration(µg/ml)	OD value	Inhibition rate%
NC	0	0.814 ± 0.377	-
1	10	0.682 ± 0.399**	16.19
2	20	0.655 ± 0.392**	19.55
3	30	0.543 ± 0.008**	33.32
4	40	0.451 ± 0.056**	44.55
5	50	0.425 ± 0.035**	47.76
6	60	0.313 ± 0.009**	60.64
7	70	0.301 ± 0.027**	61.46
8	80	0.293 ± 0.007**	64.01
9	90	0.288 ± 0.008**	64.58
10	100	0.247 ± 0.008**	69.69
Note: Compare with normal control group ** $P < 0.01$, * $P < 0.05$.			

3.3 The effects of PLE on 4T1 cell apoptosis

Compared with the normal group, 4T1 cells were treated with different concentrations of PLE (25, 50, and 100 µg/ml) for 24 h, and the number of living cells was significantly reduced (the apoptotic cells were stained orange) in a concentration-dependent manner (Fig. 1). In this study, we also assessed cell apoptosis by flow cytometry at 24 h after PLE treatment. We found that PLE significantly induced apoptosis of 4T1 cells compared with the control group (Fig. 2: A-E).

3.4 4T1 cell qRT-PCR analysis

PCR results: Bax gene expression was significantly upregulated ($P < 0.01$) and Bcl-2, ERK1/2, MEK1/2, and RAF were downregulated in the drug administration group compared with the normal control group, all of which were concentration-dependent, as shown in Fig. 3.

3.5 Effects of PLE on tumor inhibition and thymus index

PLE had a significant inhibitory effect on breast cancer, and the tumor inhibition rates were 11.65%, 33.71% and 47.24% from low dose to high dose, respectively, showing a concentration dependence. The

CTX of tumor inhibition rate was 57.74%. Tumor weight changes are shown in Fig. 4

figure 4. Effect of PLE on the tumor weight. NC: model control group, L: low dosage of PLE group ($30 \text{ mg}\cdot\text{kg}^{-1}\cdot\text{d}^{-1}$), M: medium dosage of PLE group ($60 \text{ mg}\cdot\text{kg}^{-1}\cdot\text{d}^{-1}$), H: high dosage of PLE group ($120 \text{ mg}\cdot\text{kg}^{-1}\cdot\text{d}^{-1}$), CTX: CTX group ($20 \text{ mg}\cdot\text{kg}^{-1}\cdot\text{d}^{-1}$). Compare with model group $^{##}P < 0.01, ^{\#}P < 0.05$.

The effects of each administration group on the immune organs of mice are shown in Table 3.

Table 3
The effect of PLE and CTX in mice immune organ index ($x \pm s, n = 8$)

Group	liver index($\text{mg}\cdot\text{g}^{-1}$)	Kidney index($\text{mg}\cdot\text{g}^{-1}$)	spleen index($\text{mg}\cdot\text{g}^{-1}$)	Thymus index($\text{mg}\cdot\text{g}^{-1}$)
NC	43.90 ± 1.57	11.25 ± 0.85	4.14 ± 0.36	1.85 ± 0.12
Mo	$46.92 \pm 2.42^*$	11.42 ± 0.49	$21.73 \pm 4.59^{**}$	1.70 ± 0.36
CTX	$49.55 \pm 4.91^{\#}$	12.27 ± 1.18	$17.10 \pm 2.24^{##}$	$3.18 \pm 1.90^{##}$
H	$44.05 \pm 1.31^{\#\Delta\Delta}$	$11.01 \pm 0.42^{\Delta\Delta}$	$24.97 \pm 2.42^{\Delta\Delta}$	$3.95 \pm 1.03^{##}$
M	$45.7 \pm 1.55^{\Delta\Delta}$	$10.97 \pm 1.21^{\Delta\Delta}$	$20.55 \pm 4.25^{\Delta}$	2.71 ± 1.47
L	$46.1 \pm 1.74^{\Delta}$	$10.56 \pm 0.77^{\Delta\Delta}$	20.18 ± 2.79	$2.15 \pm 0.51^{\Delta}$
Note: $^{\#}P < 0.05, ^{##}P < 0.01$ PLE group VS model group; $^{\Delta}P < 0.05, ^{\Delta\Delta}P < 0.01$ PLE group VS CTX group; $^*P < 0.05, ^{**}P < 0.01$ model group VS normal group				

Table 3 Effect of PLE in mice immune organ index. Mo: model control group, L: low dosage of PLE group ($30 \text{ mg}\cdot\text{kg}^{-1}\cdot\text{d}^{-1}$), M: medium dosage of PLE group ($60 \text{ mg}\cdot\text{kg}^{-1}\cdot\text{d}^{-1}$), H: high dosage of PLE group ($120 \text{ mg}\cdot\text{kg}^{-1}\cdot\text{d}^{-1}$), CTX: CTX group ($20 \text{ mg}\cdot\text{kg}^{-1}\cdot\text{d}^{-1}$). Compared with the model group, the renal index of PLE group mice given the drug decreased; Compared with the CTX group, the renal index of PLE group was significantly different. Compared with the model group, liver and thymus indexes were increased and spleen indexes were decreased in the CTX group; Compared with the model group, the liver index of the PLE group decreased, and the thymus and spleen indexes increased in a concentration-dependent manner.

3.6 Effect of PLE on IL-6, TNF- α , TGF- β and VEGFA levels in the serum of mice with breast cancer

The results indicated that PLE decreased the levels of IL-6, TNF- α , TGF- β and VEGFA compared with the model group and increased the levels of IL-6, TNF- α , TGF- β and VEGFA compared with the normal group (Fig. 5).

Data are presented as mean \pm SD of three experiments, n = 10. (* $P < 0.05$, ** $P < 0.01$, PLE and CTX vs model group; # $P < 0.05$, ## $P < 0.01$, model group vs normal group.)

3.7 Tumor tissue RT-PCR analysis

PCR results: Bax gene expression was significantly upregulated and Bcl-2, ERK1/2, MEK1/2, and RAF were downregulated in the drug administration group compared with the normal control group, all of which were concentration-dependent, as shown in Fig. 6.

3.8 Immunohistochemical analysis

Bax, Bcl-2 and Caspase-3 play an important role in tumor growth. Therefore, the regulation of three proteins in tumor tissues was studied by immunohistochemistry. The activation of the MAPK pathway is related to the phosphorylation of p-MEK, p-JNK and p-P38. Therefore, in this study, immunohistochemistry was used to study the regulatory effects of the three related proteins in tumor tissues. In the model group, Bax and Caspase-3 proteins were only expressed in a small number of tumor cells, and the expression of the proteins was negative. In contrast, Bax and Caspase-3 proteins were increased in each drug group, among which the expression of Bax and Caspase-3 proteins was significantly increased in the CTX group and PLE high-dose and medium-dose group, most of which were highly expressed. The expression of Bcl-2, p-MEK, p-JNK and p-P38 proteins in tumor cells was positive in the model group, and the expression of Bcl-2, p-MEK, p-JNK and p-P38 proteins in tumor tissues was reduced in all the drug groups. Among them, the protein expression of Bcl-2, p-MEK, p-JNK and p-P38 was significantly reduced in the CTX group and PLE high-dose and medium-dose groups, all of which were concentration-dependent, as shown in Fig. 7.

3.9 Effect of DMDD on the expression of MAPK signaling pathway-related proteins in mouse breast tumors

In the Western blot analysis, compared with the model group, the protein expression levels of p-ERK and p-P38 were significantly decreased in the PLE and CTX treatment groups (Fig. 8A–D).

The WB image and relative protein expression of P-ERK and P-P38. Data are presented as mean \pm SD of three experiments, n = 3. (# $P < 0.05$, ## $P < 0.01$, vs model group).

4. Discussion

In this paper, in vivo and in vitro experiments were conducted to study the effects of PLE on the proliferation and apoptosis of breast cancer cells and to preliminarily explore the antitumor effect and mechanism of the parasitic active sites of persimmon leaves. In the present study, PLE was assessed by MTT assay and exhibited potent anti-breast cancer activity in breast cancer cell lines^[13]. It inhibited the proliferation of 4T1 cells. Flow cytometry (FCM) is a common method to detect apoptosis due to its rapid, high sensitivity and quantitative properties^[14]. Flow cytometry was used to detect and analyze the effect

of PLE on the apoptosis of 4T1 cells. Flow cytometry analysis was selected for measurement of quantitative DNA content (PI staining) and apoptotic cells (double-staining fluorescent PI and annexin V-FITC)^[13]. PLE induced the apoptosis of 4T1 cells in a concentration-dependent manner.

In this study, MTT, AOEB and flow cytometry results showed that PLE inhibited the proliferation and induced the apoptosis of 4T1 breast cancer cells. Apoptosis plays an important role in inhibiting tumor growth^[15, 16]. To further explore the potential mechanism of apoptosis in 4T1 cells, PCR and immunohistochemistry were used to detect the expression of the Bax, Bcl-2 and Caspase-3 genes and proteins that may be involved in the apoptosis pathway. Tumor cells can acquire resistance to apoptosis by overexpressing antiapoptotic proteins, such as Bcl-2, and by reducing proapoptotic proteins, which are required for Cyto-c release to induce Caspase-3 activation^[17]. In this study, PLE significantly induced apoptosis in breast cancer cells by reducing Bcl-2 expression and enhancing Caspase-3 and Bax cleavage.

As a cytokine with extensive biological activity, IL-6 plays an indispensable role in the process of tumor production and progression and is involved in the differentiation, survival, apoptosis and proliferation of tumor cells^[18]. TNF- α enhances the inflammatory pathway of tumorigenesis, which in turn stimulates the proliferation of malignant cells^[19, 20]. Transforming growth factor- β (TGF- β), produced by T lymphocytes and tumor epithelial cells, is a family of protein polypeptides with a variety of functions^[21] associated with cell differentiation, growth, inflammation, damage repair, and immune regulation. TGF- β has immunosuppressive effects, enabling highly immunogenic tumor cells to escape immune surveillance and thus form tumors. VEGFA is currently one of the most active and highly specific tumor vascular-related growth factors^[22]. VEGFA is the vascular growth factor with the strongest and highest specificity in inducing tumor angiogenesis, and angiogenesis provides channels and nutrients for tumor cell migration, invasion and growth^[23]. The results showed that PLE decreased the levels of IL-6, TNF- α , TGF- β and VEGFA, suggesting that PLE enhanced the immune function of breast cancer mice to inhibit tumor growth.

The mitogen-activated protein kinase (MAPK) pathway, consisting of RAS/RAF/MEK/ERK, can transfer extracellular signals, including hormones, cytokines, and growth factors, to the nucleus, thus changing gene expression in the cell and mediating proliferation, differentiation, survival, and apoptosis^[24-28]. RAS activates at least 10 downstream signaling pathways, of which the classic one is RAS/RAF/MEK/ERK^[29, 30]. When RAF is activated on the cell membrane, it phosphorylates downstream MEK, which phosphorylates ERK, thereby producing biological effects^[24, 26, 27]. In general, promoting tumor cell apoptosis or inhibiting cell proliferation requires downregulation of the ERK and MEK signaling pathways, and lysyl oxidase peptide inhibits tumor cell proliferation and induces apoptosis by downregulating the MAPK/ERK signaling pathway^[31]. The RAF, ERK1/2 and MEK1/2 genes were downregulated by RT-PCR in vivo and in vitro in this study. Therefore, PLE may promote the apoptosis of tumor cells and inhibit the growth of breast cancer cells by interfering with the phosphorylation of ERK, JNK, MEK and RAF proteins in the MAPK signaling pathway. Further tests are needed to confirm this.

5. Conclusion

PLE enhances immunity, inhibits angiogenesis, inhibits 4T1 cell proliferation and induces apoptosis. Its apoptosis mechanism is related to the regulation of Bax/Bcl-2/Caspase-3 proteins and the phosphorylation of regulatory proteins related to the MAPK signaling pathway.

Abbreviations

Bax	Bcl-2 associated X protein
Bcl-2	B-cell lymphoma-2
Caspase-3	Cysteine proteases with aspartate specificity-3
DAPI	4',6-diamidino-2-phenylindole
PLE	ethyl acetate extract from persimmon leaves
RPMI1640	Roswell Park Memorial Institute
FBS	Fetal Bovine Serum
DMSO	Dimethyl Sulfoxide
FCM	Flow cytometry
FITC	Fluorescein Isothiocyanate
CTX	Cyclophosphamide endoxan cytoxan
ELISA	Enzyme-Linked Immunosorbent Assay
ERK	Extracellular regulated protein kinases
h	hour
HE	Hematoxylin and Eosin
IL-6	Interleukin-6
JNK	c-Jun N-terminal kinase
MAPK	Mitogen-activated protein kinase
MEK	Mitogen activated protein kinase
min	minute
mRNA	Messenger RNA
PBS	Phosphate buffer saline
RAF1	Proto oncogene serine / threonine protein kinase
rpm	round per mineter
RT-qPCR	Real-time quantitative polymerase chain reaction
TGF- β 1	Transforming growth factor- β 1
TNF- α	Tumor necrosis factor
VEGF	Vascular endothelial growth factor
WB	Western blotting

Declarations

Acknowledgements

This study was funded by Natural Science Foundation of China (No. 81760665, 81460205), the Guangxi Key Laboratory of Bio-targeted Diagnosis, Treatment Research (No. GXSWBX201804) and Guangxi first-class discipline project for pharmaceutical sciences (No. GXFCDP-PS-2018).

Author's Contributions

1) Name Fang Zhuge E-mail: 1055755630@qq.com █design of the work█the acquisition, analysis█ interpretation of data█have drafted the work

2) Name Xiusha Wei E-mail: 1336794269@qq.com█design of the work

3)Name Yani Wu E-mail: 1159475237@qq.com█the acquisition,

4)Name Guining Wei E-mail: weiguining@163.com█the acquisition, 5)Name Chen Ming E-mail:chenmingcm@163.com█analysis

6)Name Yutong Gao E-mail: 591090229@qq.com█analysis

7)Name Zhaoni Chen E-mail:wonderyao@163.com█the creation of new software used in the work

8)Name Xiaolin Zhang E-mail:zxlzxl420@163.com█the creation of new software used in the work

9)Name Shunyu Lu E-mail:nnlsy2010@163.com█the creation of new software used in the work

Corresponding author:

Name: Renbin Huang E-mail: huangrenbin518@163.com█design of the work

Name: Xiuneng Tang E-mail: zhugexiaozhu@163.com█design of the work

Competing interests

The authors declare that they have no known competing financial interests or personal relationships that could have appeared to influence the work reported in this paper.

Consent to publish

I understand that the information will be published in Chinese Medicine, but that full anonymity cannot be guaranteed.I understand that the text and any pictures or videos published in the article will be freely available on theinternet and may be seen by the general public. The pictures, videos and text may also appear on other websitesor in print, may be translated into other languages or used for commercial purposes.I have been offered the opportunity to read the manuscript.

Signing this consent form does not remove my rights to privacy

Funding

This study was funded by Natural Science Foundation of China (No. 81760665, 81460205), the Guangxi Key Laboratory of Bio-targeted Diagnosis, Treatment Research (No. GXSWBX201804) and Guangxi first-class discipline project for pharmaceutical sciences (No. GXFCDP-PS-2018).

References

1. Fitzmaurice C, Dicker D, Pain A, et al. The global burden of cancer 2013, *JAMA onco.* 2015,1: 505–527.
2. Siegel RL, Miller KD, Jemal A. Cancer. *Cancer statistics, 2019, CA A. J Clin.* 2019;69(1):7–34.
3. Bray F, Ferlay J, Soerjomataram I, et al. Global cancer statistics 2018: GLOBOCAN estimates of incidence and mortality worldwide for 36 cancers in 185 countries, *CA A Cancer. J. Clin.* 2018,68:394–424.
4. Gao Ying, Huang Renbin, Gong Yixuan. et al. The antidiabetic compound 2-dodecyl-6-methoxycyclohexa-2,5-diene-1,4-dione, isolated from *Averrhoa carambola* L. demonstrates significant antitumor potential against human breast cancer cells [J] *Oncotarget.* 2015;6:24304–19.
5. Siriphorn Chimolee P, Graidist T, Srisawat, et al. Anti-breast cancer potential of frullanolide from *Grangea maderaspatana* plant by inducing apoptosis. [J]. 2019,6:5283–5291.
6. Ding Y, Kai R, Huanhuan D, et al. Flavonoids from persimmon (*Diospyros kaki* L.) leaves inhibit proliferation and induce apoptosis in PC-3 cells by activation of oxidative stress and mitochondrial apoptosis. [J] *Chem Biol Interact.* 2017;275:210–7.
7. Kawakami K. Persimmon leaf flavonols enhance the anti-cancer effect of heavy ion radiotherapy on murine xenograft tumors. [J]. *Cancer Ther.* 2013;4:1150–7.
8. LingWD DuG. Effect of flavonoid from *diospyros kaki* leaves on TGF- β 1 and MMP-9 in blood glucose levels and kidney tissues of rats with diabetic nephropathy. *Chin [J] Exp Tradit Med Form.* 2016;22:139–43.
9. SunL ZhangJ. LuX, et al. Evaluation to the antioxidant activity of total flavonoids extract from persimmon (*Diospyros kaki* L.) leaves. *Food Chem. Toxic.* 2011,49:2689–2696.
10. Zhang Y, WangS, Hao M, et al. Study on the effect and the anti-inflammatory mechanisms of persimmon leaf flavonoid in the treatment of experimental oral ulcer. *China Prac. Med.* 2017,12:185–187.
11. YinSL. The effect of persimmon flavone on spores number and antibacterial activity of BSD-2. [J]. *Microbiol.* 2010,30:47–50.
12. KawakamiK. Antihypertensive and vasorelaxant effects of water-soluble proanthocyanidins from persimmon leaf tea in spontaneously hypertensive rats. *Biosci. Biotech. Bioch.* 2011,75:1435–1439.

13. Siriphorn Chimolee P, Graidist T, Srisawat, et al. Anti-breast cancer potential of frullanolide from *Grangea maderaspatana* plant by inducing apoptosis.[J].2019;6:5283–5291.
14. Mitsis M, Alexiou GA, Vartholomatos E, et al. N-(p-coumaroyl) serotonin induces cell cycle arrest and apoptosis in breast cancer cells [J]. *Journal of BUON*. 2018;23(1):129–33.
15. J. Lopez.,Mitochondrial apoptosis: killing cancer using the enemy within, *Br.J. Cancer* 112,2015, 957.
16. Hassan M. Apoptosis and molecular targeting therapy in cancer, *Biomed Res.Int*. 2014, 2014.
17. Renault TT. Mitochondrial shape governs BAX-induced membrane permeabilization and apoptosis, *Mol. Cell*,2015,57:69–82.
18. Taniguchi K, Karin M. IL-6 and related cytokines as the critical lynchpins between inflammation and cancer[J]. *Semin Immunol*. 2014;26(1):54–74.
19. Murata M,Thanan R,Ma N,et al.Role of nitrate and oxidative DNA damage in inflammation-related carcinogenesis [J].*J Biomed Biotechnol*,2012,2012(10) : 623019.
20. Wei Z, Cao S, Liu S,et al.Could gut microbiota serve as prognostic biomarker associated with colorectal cancer patients' survival? A pilot study on relevant mechanism [J].*Oncotarget*,20167(29): 46158–46172.
21. Katz MS, Thatch KA, Schwartz MZ. Hepatocyte growth factor and omega-3-enriched feeds have a synergistic effect on mucosal mass in an animal model of inflammatory bowel disease [J].*J Pediatr Surg*,2012,47(1) : 194–198.
22. Bueno MJ, Mouron S, Quintela-Fandino M. Personalising and targeting antiangiogenic resistance: a complex and multifactorial approach[J]. *Br J Cancer*. 2017;116(9):1119–25.
23. Chen T, You Y, Jiang H, et al. Epithelial-mesenchymal transition (EMT): A biological process in the development, stem cell differentiation, and tumorigenesis. *J Cell Physiol*. 2017;232(12):3261–72.
24. Cantwell-Dorris ER, O'Leary JJ, Sheils OM. BRAFV600E: implications for carcinogenesis and molecular therapy[J]. *Mol Cancer Ther*. 2011;10(3):385–94.
25. Lito P, Rosen N, Solit DB. Tumor adaptation and resistance to RAF inhibitors[J]. *Nat Med*. 2013;19(11):1401–9.
26. Burotto M, Chiou VL, Lee JM, et al. The MAPK pathway across different malignancies: a new perspective[J]. *Cancer*. 2014;120(22):3446–56.
27. Hall RD, Kudchadkar RR. BRAF mutations: signaling, epidemiology, and clinical experience in multiple malignancies[J]. *Cancer Control*. 2014;21(3):221–30.
28. Michaloglou C, Vredeveld LC, Mooi WJ, Peeper DS. BRAF(E600)in benign and malignant human tumours[J]. *Oncogene*. 2008;27(7):877–95.
29. Santarpia L, Lippman SM, El-Naggar AK. Targeting the MAPK-RAS-RAF signaling pathway in cancer therapy[J]. *Expert Opin Ther Targets*. 2012;16(1):103–19.
30. Vakiani E, Solit DB. KRAS and BRAF: drug targets and predictive biomarkers[J]. *J Pathol*. 2011;223(2):219–29.

31. Zheng Y, Wang X, Wang H, Yan W, Zhang Q, Chang X. Expression of the lysyl oxidase propeptide in hepatocellular carcinoma and its clinical relevance. *Oncol Rep.* 2014;31:1669–76.

Figures

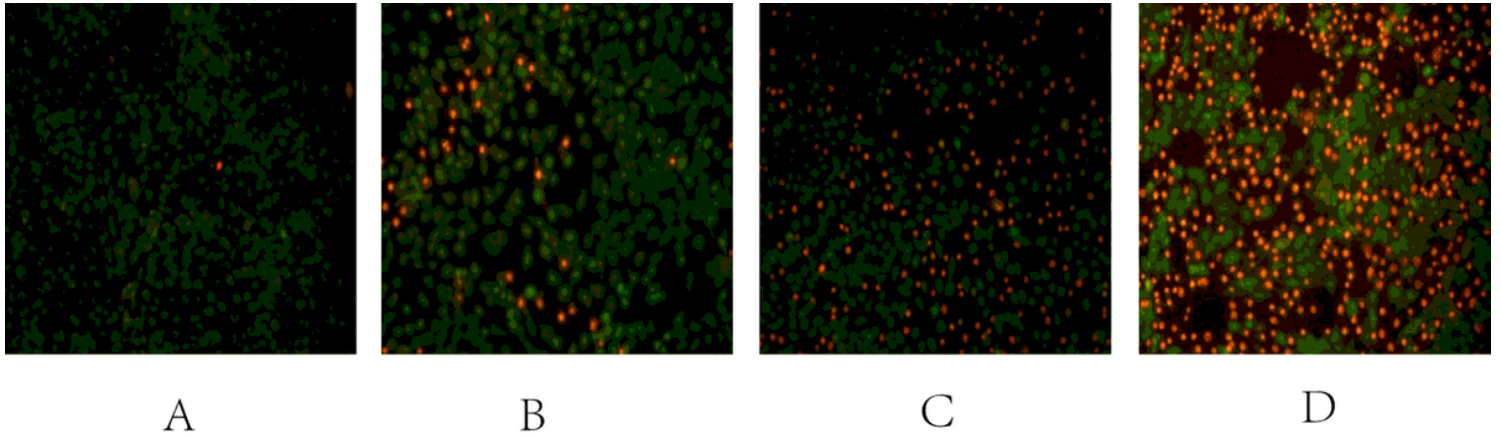


Figure 1

The effect of PLE on 4T1 cells apoptosis. A:normal control group, B:low dosage of PLE group(25µg/ml), C:medium dosage of PLE group(50µg/ml), D:high dosage of PLE group(100µg/ml).

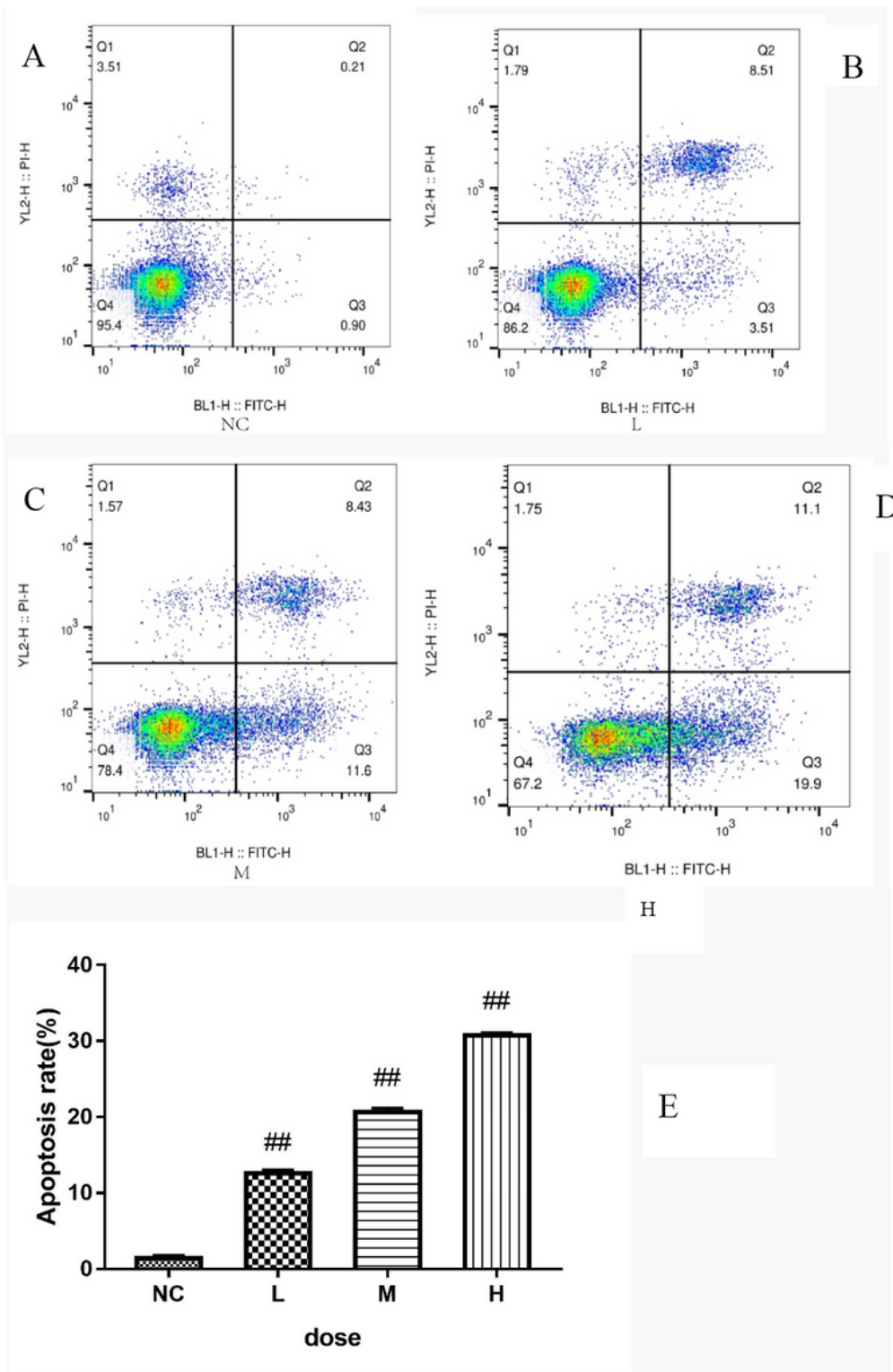


Figure 2

The cell of apoptosis rate for the AnnexinV-FITC/PI flow cytometry analysis by treating the cells with different concentrations of PLE. A(NC): normal control group, B(L): low dosage of PLE group(25 μ g/ml), C(M): medium dosage of PLE group(50 μ g/ml), D(H): high dosage of PLE group(100 μ g/ml). E stands for flow cytometry to detect the apoptosis rate of different concentrations of PLE. The data are presented as the mean \pm SD (n=3). #P < 0.05, ##P < 0.01 compared to the normal control group.

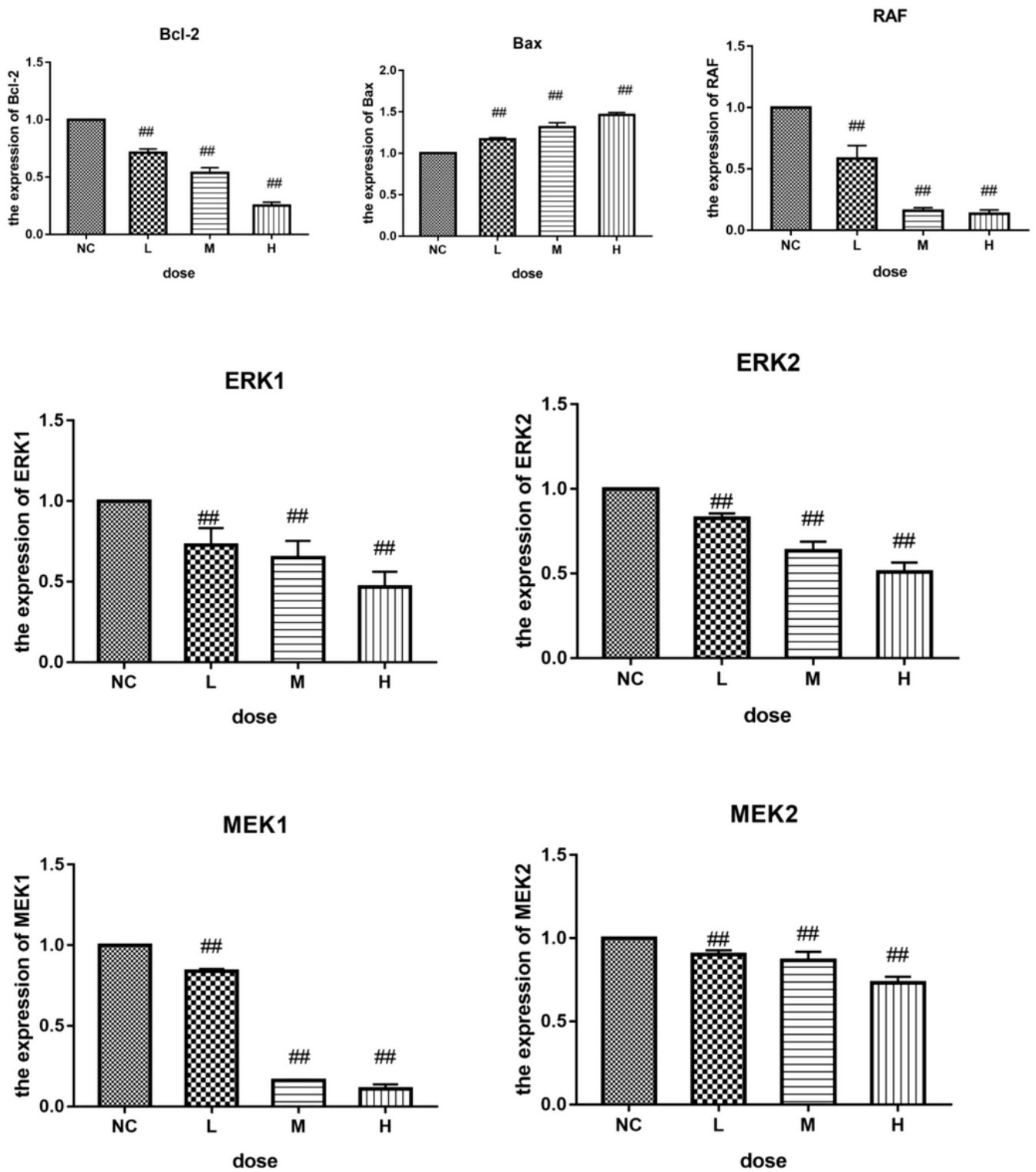


Figure 3

Effect of PLE on the mRNA levels of Bax, Bcl-2, ERK1/2, MEK1/2, and RAF. NC: normal control group, L: low dosage of PLE group (25 μg/ml), M: medium dosage of PLE group (50 μg/ml), H: high dosage of PLE group (100 μg/ml). Compare with normal control group ##P < 0.01, #P < 0.05.

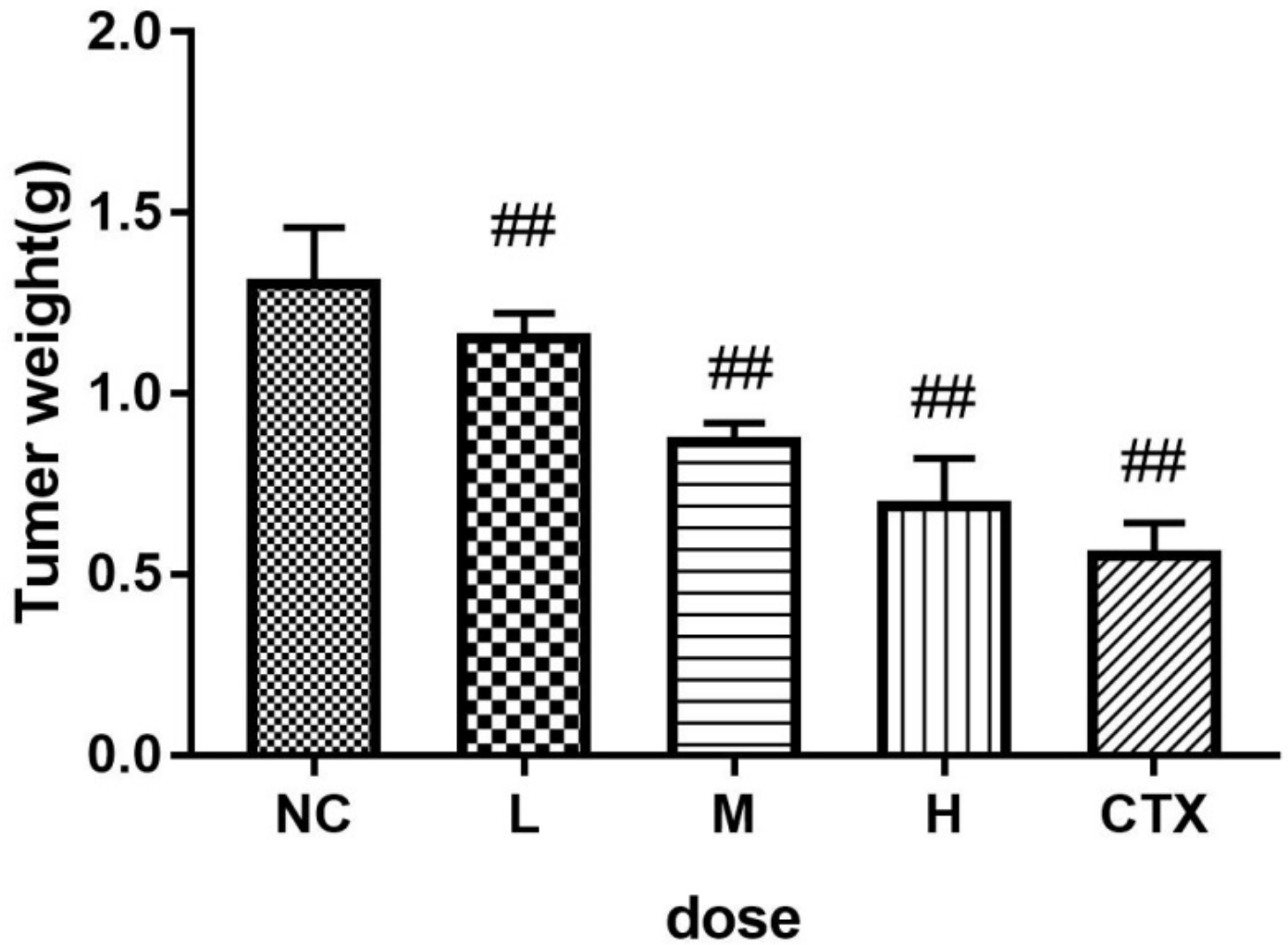


Figure 4

Effect of PLE on the tumor weight. NC: model control group, L: low dosage of PLE group (30mg.kg⁻¹.d⁻¹), M: medium dosage of PLE group (60mg.kg⁻¹.d⁻¹), H: high dosage of PLE group (120mg.kg⁻¹.d⁻¹), CTX: CTX group (20mg.kg⁻¹.d⁻¹). Compare with model group ##P<0.01, #P<0.05.

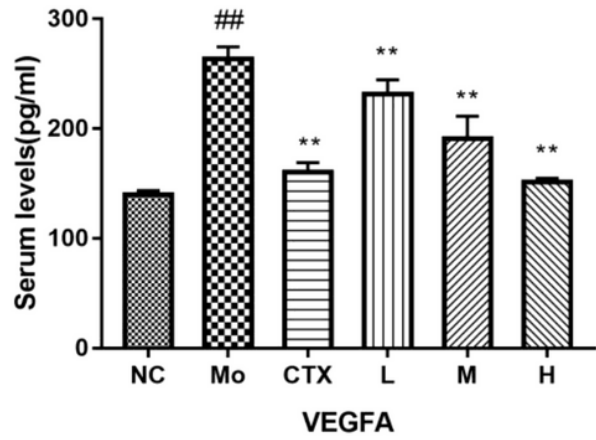
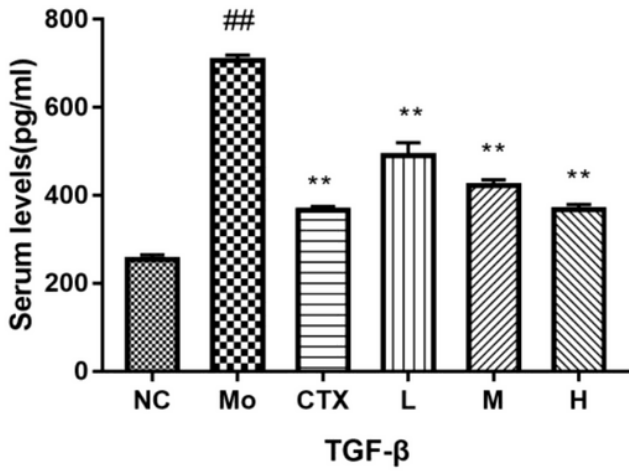
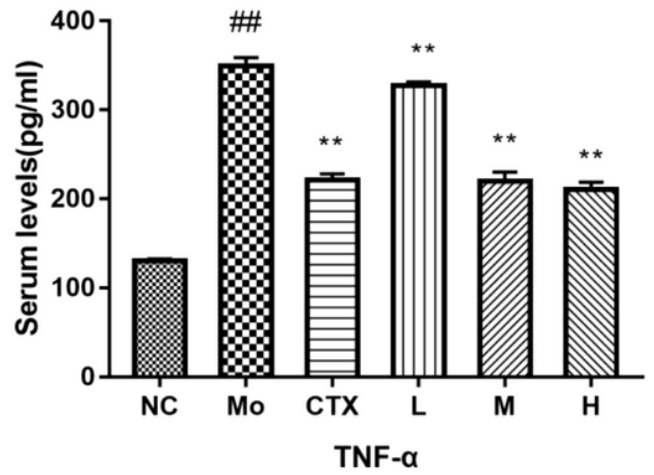
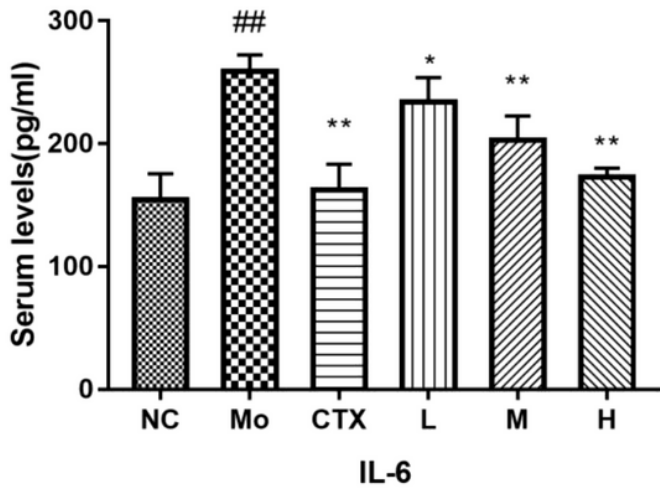


Figure 5

The effect of PLE on cytokines in breast cancer mice. NC: normal control group .Mo: model control group, L: low dosage of PLE group(30 mg.kg⁻¹.d⁻¹), M: medium dosage of PLE group(60 mg.kg⁻¹.d⁻¹), H: high dosage of PLE group(120 mg.kg⁻¹.d⁻¹), CTX: CTX group(20 mg.kg⁻¹.d⁻¹) .

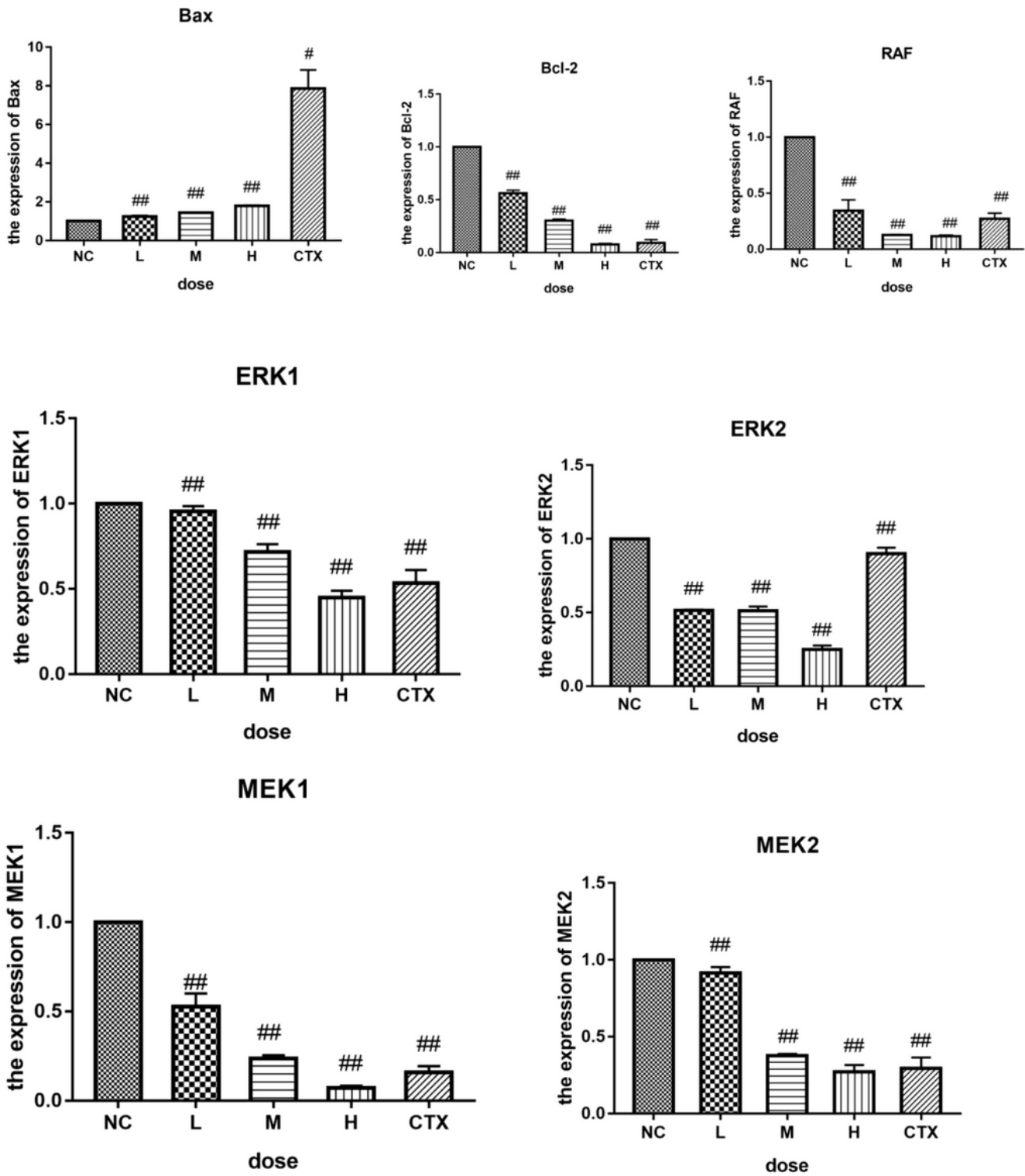


Figure 6

Effect of PLE on the mRNA levels of Bax, Bcl-2, ERK1/2, MEK1/2, and RAF. NC: model control group, L: low dosage of PLE group (25 μg/ml), M: medium dosage of PLE group (50 μg/ml), H: high dosage of PLE group (100 μg/ml). Compare with normal control group ##P < 0.01, #P < 0.05.

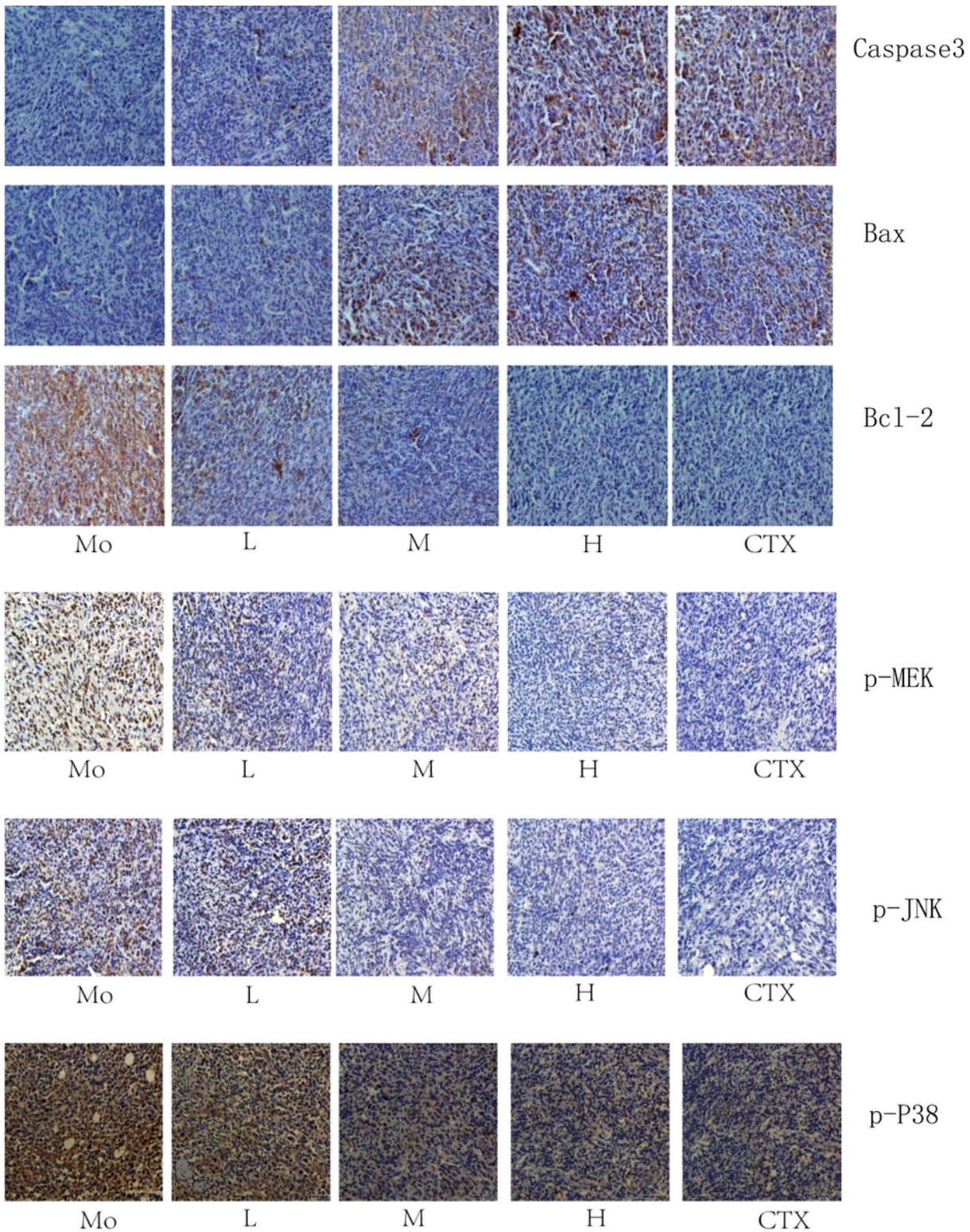


Figure 7

Effects of PLE on Bax, Caspase3 and Bcl-2, p-MEK, p-JNK and p-P38 proteins expression in transplanted tumor tissues. Mo: model group, L:low dosage of PLE group(30mg.kg⁻¹.d⁻¹), M:medium dosage of PLE group(60mg.kg⁻¹.d⁻¹), H:high dosage of PLE group(120mg.kg⁻¹.d⁻¹).CTX:CTX group(20 mg.kg⁻¹.d⁻¹).

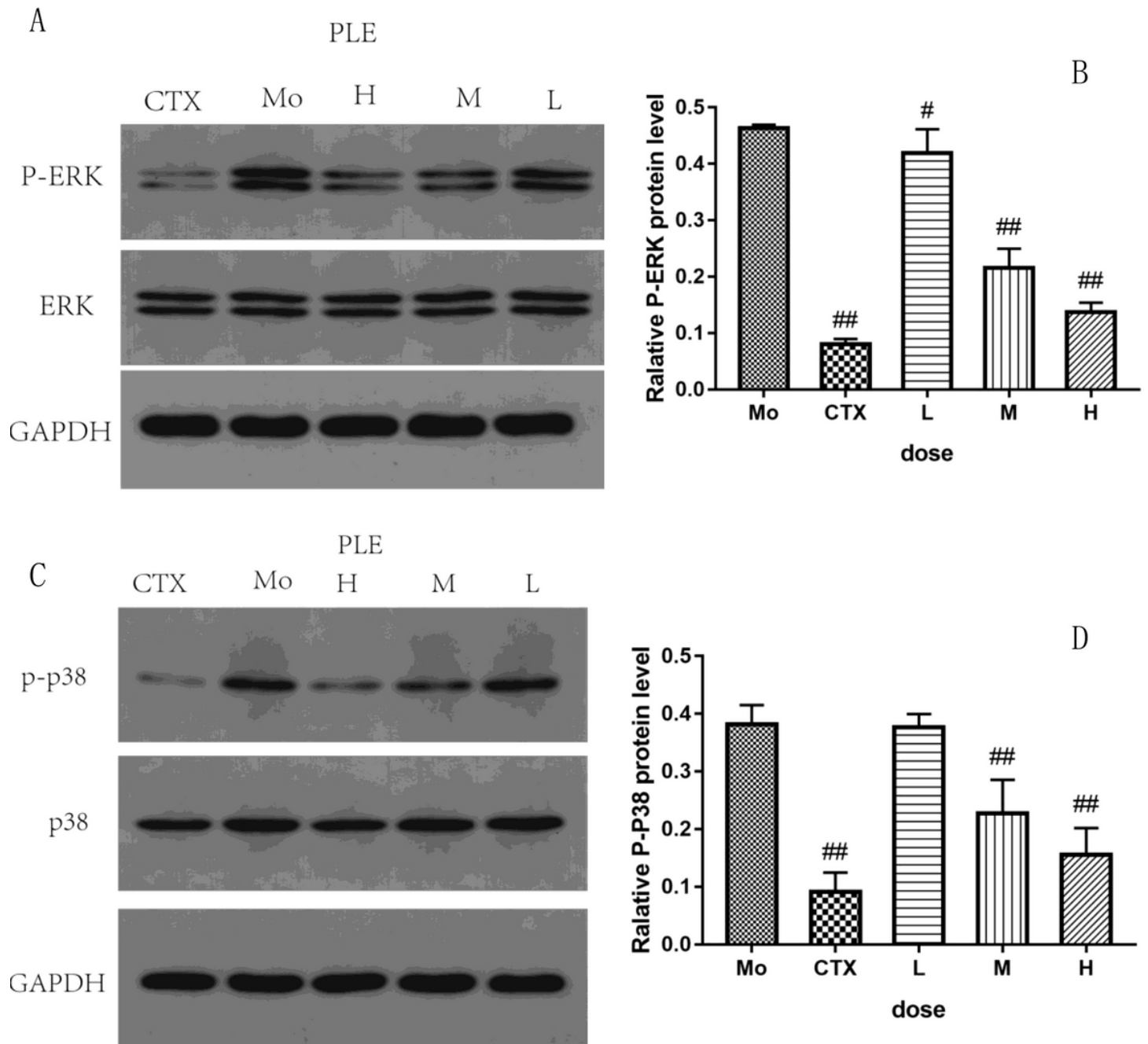


Figure 8

Effects of PLE on P-ERK and P-P38 protein expression in transplanted tumor tissues. Mo: model group, L:low dosage of PLE group(30mg.kg-1.d-1), M:medium dosage of PLE group(60mg.kg-1.d-1), H:high dosage of PLE group(120mg.kg-1.d-1).E:CTX group(20 mg.kg-1.d-1).